PHASED ARRAY FOR MULTI-DIRECTION SECURE COMMUNICATION

M.P. Daly and J.T. Bernhard
Electromagnetics Laboratory
University of Illinois at Urbana-Champaign
Urbana, IL 61801
mpdaly@illinois.edu, jbernhar@illinois.edu

Abstract: A digital modulation technique, which we will call directional modulation, is presented. Directional modulation uses the array elements to modulate a continuous wave (CW) signal rather than implement modulation in the transmitter hardware. By switching an array of reconfigurable elements, arbitrary amplitudes and phases of radiation patterns can be achieved. Because this signal is direction-dependent, the technique offers security as the signal will become distorted off the desired direction, and it makes possible sending independent data in multiple directions. When using an array with driven elements, the necessary configurations can be predicted from simple calculations instead of having to test all possible combinations experimentally or rely on complex simulation software. The experimental methods and results of different modulation schemes are presented.

1. Introduction

In a conventional phased array, information bits are converted into a baseband IQ modulation. The baseband signal is then upconverted by mixing with a carrier frequency, and the RF signal goes through a feeding network, phase shifters, amplifiers, and finally the antenna elements. Using constructive interference, a phased array improves the gain of a radiated signal in the direction of the receiver while suppressing radiation in undesired directions. But even though a phased array may have many elements, it can only transmit one stream of data at a time. This signal is radiated in other directions than the intended one, with a decrease in gain according to the sidelobe levels. However, a sufficiently sensitive receiver in some other undesired direction can still decode the same signal from the array.

Time-modulated arrays make use of an additional dimension, time, in the design of high performance arrays. In these arrays, elements are usually switched on and off in a

periodic manner for such goals mimicking an amplitude taper [1] or rotating the phase center of the array to move sidelobes out of the pass band [2], [3].

Instead of switching elements simply for radiation pattern synthesis, several groups have proposed sending information by modulating the array elements. These techniques can be used to deliver frequency shift keying [4], pulse-position modulation [5], or amplitude and phase-based modulations [6]. In [4]–[6], the element modulation not only produces the array pattern but also conveys the information.

The modulations produced in [4]-[6] have a spatial component, hence the name directional modulation. They appear distorted to receivers not in the intended transmit direction, making demodulation more difficult or even impossible. Directional modulation can be accomplished using reconfigurable elements, phase shifters, or dynamic attenuation, with data speeds dependent on the switching speeds of these devices. At minimum, the elements need only be driven by a CW signal. A block diagram illustrating the differences between conventional array transmission and directional modulation, in this case using reconfigurable elements, is shown in Figure 1.

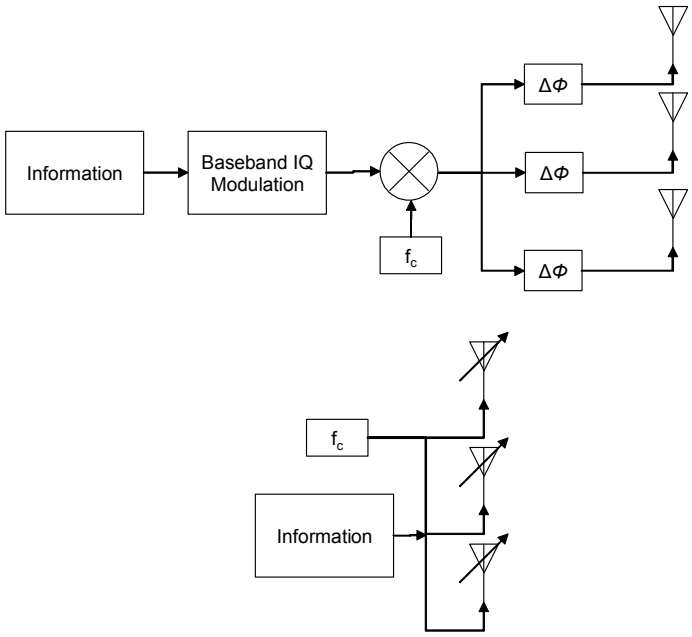

Figure 1: Simplified model of traditional array in transmit mode (left) and one implementation of a directional modulation transmitter using reconfigurable elements (right)

Recently, a parasitic array was demonstrated that could generate modulated signals that were directionally-dependent [6]. The parasitic array consisted of a single driven planar dipole surrounded by switched parasitic elements. The switches on the parasitics were used to alter the amplitude and phase of the radiated signal for a given direction. This

array was successful in obtaining quadrature amplitude modulation (QAM) but there was no easy way to determine the switch combination that would synthesize a given constellation point. Because it was a parasitic array, there was no way given to accurately predict the magnitude and phase of radiated fields from a specific switch combination of the 90 switches in the array, short of running a time-consuming electromagnetic simulation.

However, when an array is composed entirely of driven elements, it will be shown in this work that the total radiated field can be predicted without complex simulations if the active element patterns are known. An active element pattern is an element's radiation pattern while operating in the array rather than the isolated element. It takes into account mutual coupling effects. Because Maxwell's equations are linear, the total pattern of the array is a superposition of the active element patterns multiplied by phase offsets for their positions in the array. Using this method, the same benefits of multi-directional communications and secure, directionally-dependent modulation can be realized, and an array can be designed with more intuition and less complexity. Basic mathematics behind directional modulation will be presented first, followed by a description of the experimental setup. Finally, the results of several different modulation tests will be presented, with comparisons between calculated and measured data.

2. Mathematical Theory

The array factor for a linear, uniformly spaced array can be defined as [7]:

$$\mathrm{A}(\varphi)=\sum_{n=1}^{N}\mathrm{H_n}(\varphi)\exp\left(\frac{\mathrm{j}2\pi(\mathrm{n}-1)\mathrm{d}\sin(\varphi)}{\lambda}\right) \tag{1}$$

where $H_n(\varphi)$ is the complex active element radiation pattern of element n, d is the inter-element spacing, N is the number of elements in the array, and λ is the wavelength. The total pattern including phase information is then given by $A(\varphi)$. If the amplitude or phase of each element can be manipulated, then the amplitude and phase of a signal in direction φ from the array can be controlled. In fact, there are N degrees of freedom for controlling the transmitted signal in one direction. If instead it is desired to specify magnitude and phase in N different directions, the required weightings and phase shifts can be solved by means of a simple linear system of equations:

$$\begin{bmatrix} A(\varphi_1) \\ A(\varphi_2) \\ \vdots \\ A(\varphi_N) \end{bmatrix} = \begin{bmatrix} H_1(\varphi_1)\cdot e^{j\frac{2\pi\cdot 0\cdot d\sin\varphi_1}{\lambda}} & H_2(\theta_1)\cdot e^{j\frac{2\pi\cdot 1\cdot d\sin\varphi_1}{\lambda}} & \cdots & H_N(\varphi_1)\cdot e^{j\frac{2\pi\cdot(N-1)\cdot d\sin\varphi_1}{\lambda}} \\ H_1(\varphi_2)\cdot e^{j\frac{2\pi\cdot 0\cdot d\sin\varphi_2}{\lambda}} & H_2(\theta_2)\cdot e^{j\frac{2\pi\cdot 1\cdot d\sin\varphi_2}{\lambda}} & \cdots & H_N(\varphi_2)\cdot e^{j\frac{2\pi\cdot(N-1)\cdot d\sin\varphi_2}{\lambda}} \\ \vdots & & \ddots & \vdots \\ H_1(\varphi_N)\cdot e^{j\frac{2\pi\cdot 0\cdot d\sin\varphi_N}{\lambda}} & H_2(\theta_N)\cdot e^{j\frac{2\pi\cdot 1\cdot d\sin\varphi_N}{\lambda}} & \cdots & H_N(\varphi_N)\cdot e^{j\frac{2\pi\cdot(N-1)\cdot d\sin\varphi_N}{\lambda}} \end{bmatrix} \cdot \begin{bmatrix} x_1 \\ x_2 \\ \vdots \\ x_N \end{bmatrix} \tag{2}$$

The vector $[x_1 \ldots x_N]^T$ is a vector of complex weights, which could correspond to phase shifts and changes in amplitude weighting of elements. When solving (2), it is assumed the elements have full freedom to change their phase and weighting. Often, this is impractical and optimization methods are needed to find the best solution using only phase shifters, for example.

In this work, directional modulation is implemented using driven elements which generate constellation points according to (2). The equation (2) can easily be generalized to any arbitrarily-spaced array by changing the phase terms, but this work will focus on a four-element linear array with uniform spacing. The array in this work has reconfigurable elements and does not have phase shifters or variable attenuators. Each element can reconfigure between two pattern states, so it would be more accurate to write (2) in the following manner:

$$\begin{bmatrix} A(\varphi_1) \\ A(\varphi_2) \\ \vdots \\ A(\varphi_N) \end{bmatrix} = \begin{bmatrix} f(\varphi_1)\cdot e^{j\frac{2\pi\cdot 0\cdot d\sin\varphi_1}{\lambda}} & f(\varphi_1)\cdot e^{j\frac{2\pi\cdot 1\cdot d\sin\varphi_1}{\lambda}} & \cdots & f(\varphi_1)\cdot e^{j\frac{2\pi\cdot (N-1)\cdot d\sin\varphi_1}{\lambda}} \\ f(\varphi_2)\cdot e^{j\frac{2\pi\cdot 0\cdot d\sin\varphi_2}{\lambda}} & f(\varphi_2)\cdot e^{j\frac{2\pi\cdot 1\cdot d\sin\varphi_2}{\lambda}} & \cdots & f(\varphi_2)\cdot e^{j\frac{2\pi\cdot (N-1)\cdot d\sin\varphi_2}{\lambda}} \\ \vdots & & \ddots & \vdots \\ f(\varphi_N)\cdot e^{j\frac{2\pi\cdot 0\cdot d\sin\varphi_N}{\lambda}} & f(\varphi_N)\cdot e^{j\frac{2\pi\cdot 1\cdot d\sin\varphi_N}{\lambda}} & \cdots & f(\varphi_N)\cdot e^{j\frac{2\pi\cdot (N-1)\cdot d\sin\varphi_N}{\lambda}} \end{bmatrix} \cdot \begin{bmatrix} H_{1,i_1} \\ H_{2,i_2} \\ \vdots \\ H_{N,i_N} \end{bmatrix} \quad (3)$$

H_{1,i_1} indicates the entire active element pattern of element 1 where i_1 can either be a 0 or a 1 representing the two states, broadside and endfire, of the element. $f(\varphi_i)$ is a selector function whose product with the element pattern produces the value of the radiation pattern at φ_i, as shown in (4):

$$H_{n,k_n}(\varphi_m) = f(\varphi_m) H_{n,k_n} \quad (4)$$

In the four-element array discussed in this work, there are only 16 possible transmitted signals for a given direction, so optimization methods for obtaining desired signals are less practical than simply calculating all possible values once the array matrix and the H vector in (3) are known. But (3) serves to illustrate that this type of an array has easily calculable constellation points once the element patterns are known. Instead of having to calculate all possible combinations of switches which is exponential in complexity, only the active element patterns have to be simulated or measured, which is linear in complexity.

3. Experimental Setup

3.1 Reconfigurable Antenna Array

The array used in all subsequent experiments is a 4 element linear array with half-wavelength spacing shown in Figure 2. The elements are reconfigurable square spiral microstrip antennas outlined in [8]. The array was created initially to assess beamsteering capabilities using reconfigurable elements [9]. This array uses ideal switches (copper tape) rather than RF MEMS to switch between two modes. The switch locations are highlighted on the first element in Figure 2.

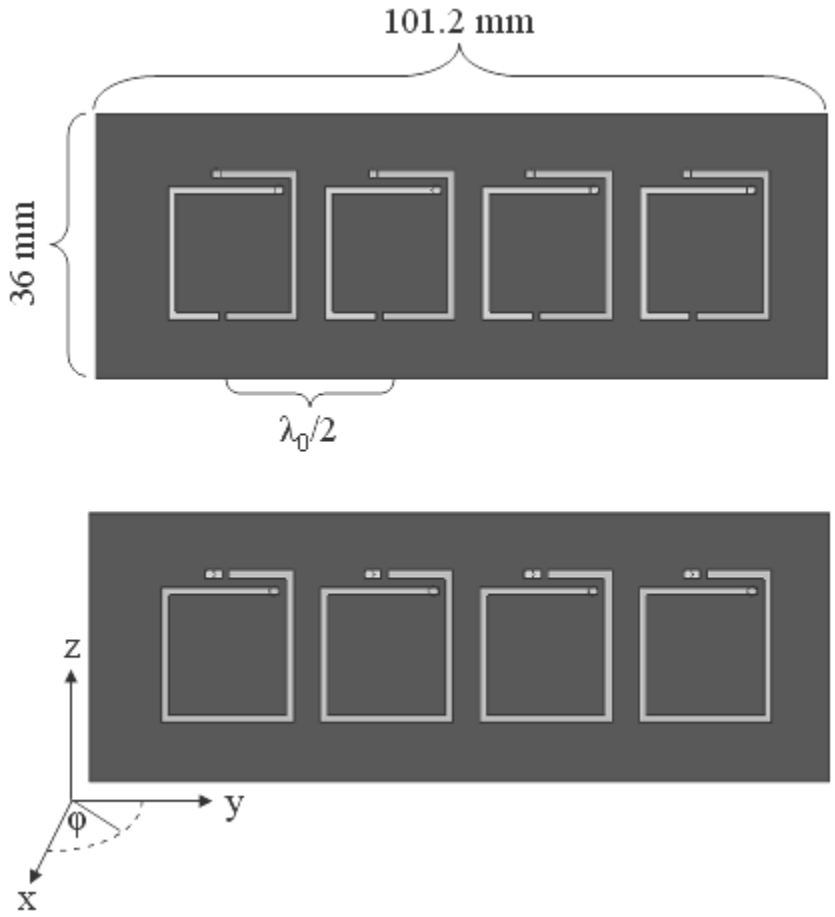

Figure 2: Reconfigurable 4x1 array [9]. All elements in broadside mode (top) and endfire mode (bottom) .

To reconfigure an element to broadside, the top switch location shown in Figure 2 is closed and the bottom is opened. To achieve endfire radiation, the top switch is open and the bottom is closed. The impedance match for each element was measured for both modes, and all elements have a VSWR of less than 2 at the operating frequency of 6.9 GHz. This is illustrated in Figure 3. The mode (broadside or endfire) of an element's neighbors had no significant effect on the measured impedance or radiation pattern of the element.

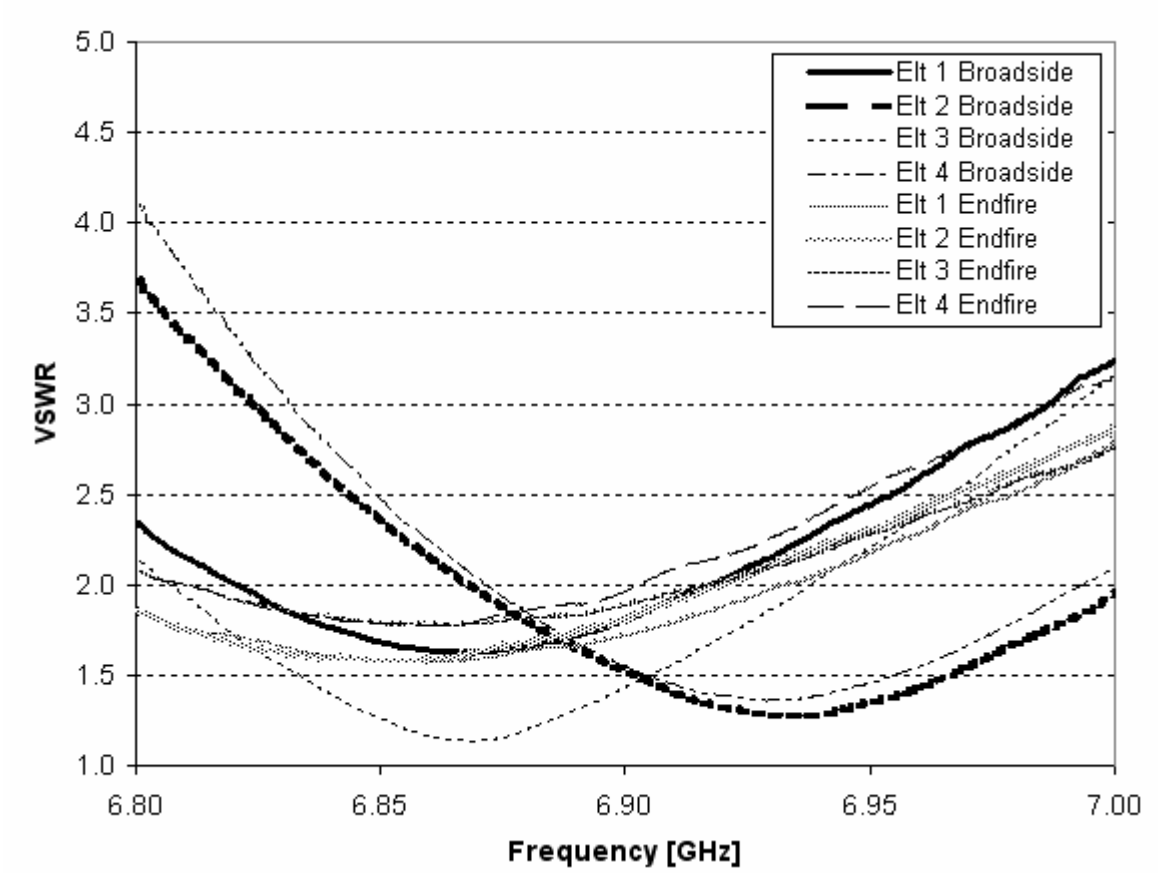

Figure 3: Measured VSWR of array elements

3.2 Active Element Pattern Measurement

In order to accurately predict the constellation points for a given configuration, the active element patterns of each element must be known. As mentioned earlier, the active element patterns are radiations patterns of the individual elements when operating in the array. These patterns were taken by terminating all the other elements with matched loads. Figure 4 shows the broadside and endfire patterns of each element for vertical polarization only (from Figure 2, the array was rotated in φ and the vertical polarization was measured). The endfire patterns have nulls at approximately 0° (array broadside) and the broadside patterns have maxima closer to 25°. The horizontal polarization has a maximum closer to 0° in broadside mode, but for this application, the broadside maximum does not have to be exactly at 0°.

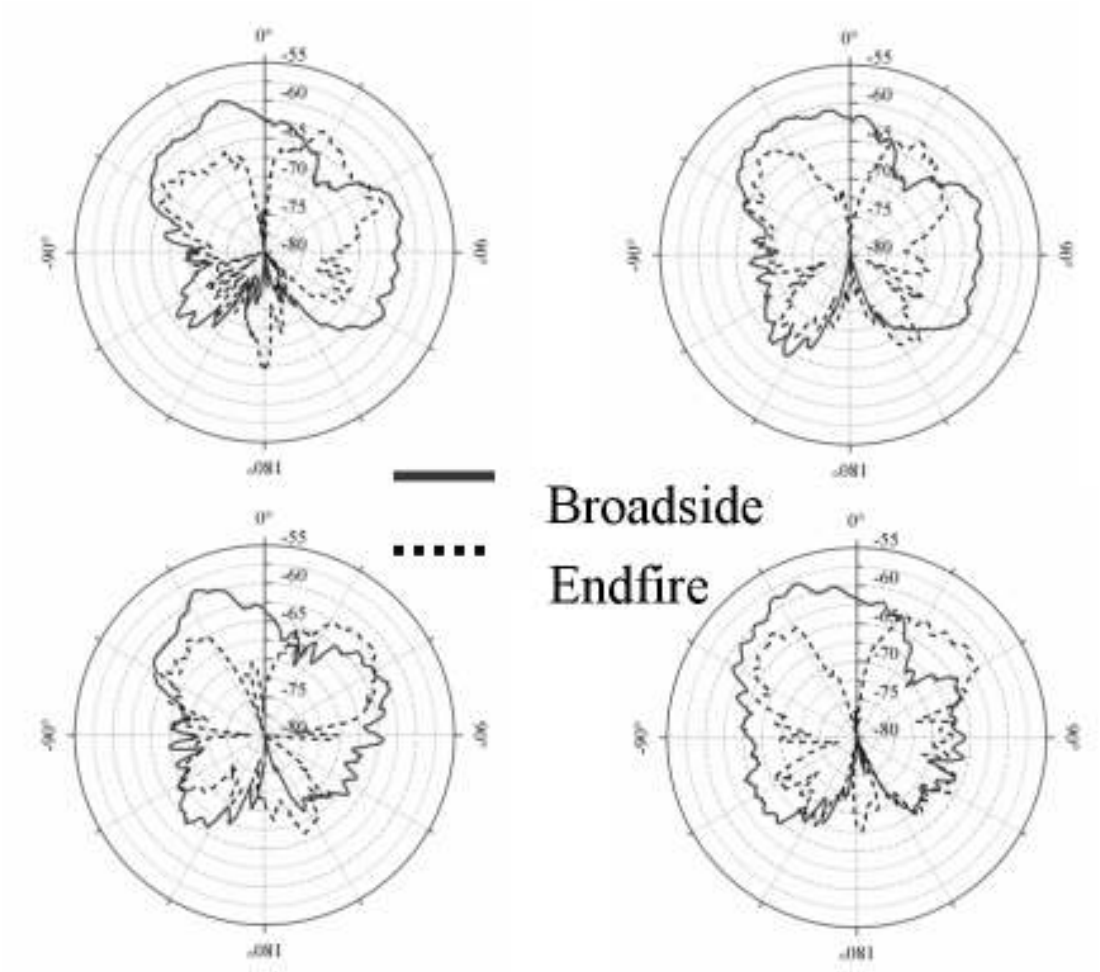

Figure 4: Individual element patterns (θ=90° plane). Vertical (z direction) polarization only (see Figure 2). Elements 1&2 on top row, 3&4 on bottom row.

It is interesting to note that while the magnitude of the broadside and endfire patterns are very different, the relative phases of the elements are approximately the same. Figure 5 shows the phases of each element pattern in both modes. Figure 5 does not include the relative phase difference due to element position in the array.

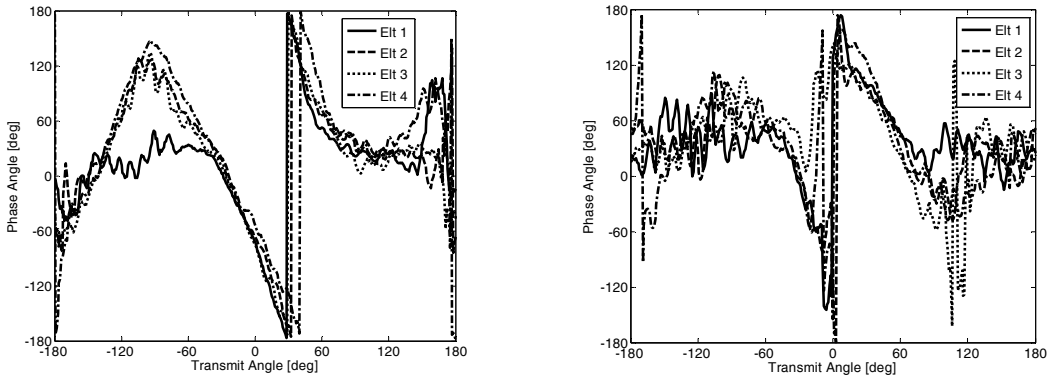

Figure 5: Phase of elements 1-4 in broadside mode (left) and endfire mode (right)

4. Experimental Results

4.1 Prediction of the Array Pattern from Active Element Patterns

This section will demonstrate the accuracy of predicting the total pattern from individual element patterns. Figure 6 shows the radiation patterns when all 4 elements are driven in either broadside or endfire mode. The magnitudes are duplicated again in Figures 7 and 8, which also shown the phases.

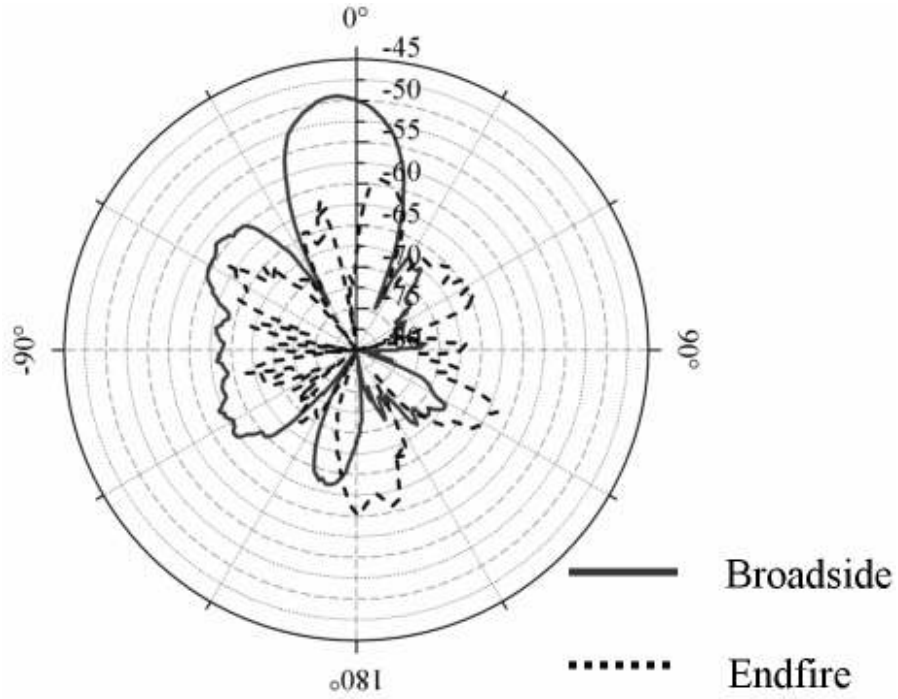

Figure 6: Combined pattern with all elements in either broadside mode or endfire mode. Vertical polarization only (see Figure 2) in the θ=90° plane.

Figures 7 shows the predicted and measured patterns when all of the elements are in broadside mode and Figure 8 shows the same measurements when all of the elements are in endfire mode. The predicted values are calculated from simply adding up the individual element patterns taken in broadside or endfire mode. As can be seen, the predicted magnitude and phase agree well with the measured data. As a side note, because the switches were hard-wired, the array had to be removed from the testing apparatus to switch elements between broadside and endfire. Care was taken to stabilize the testing apparatus so the position of the array in space was preserved. The phase is especially sensitive at this frequency as a change in relative position of 1 mm means a phase change of almost 10°. The largest deviations between measured and predicted occurred when the signal strength was very low, which was likely due to system noise.

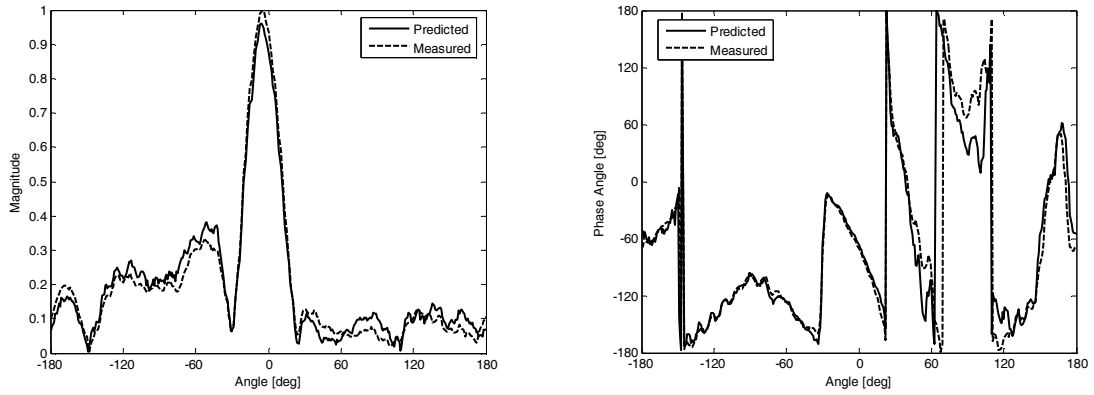

Figure 7: Predicted and measured pattern magnitude and phase when all elements are in broadside mode

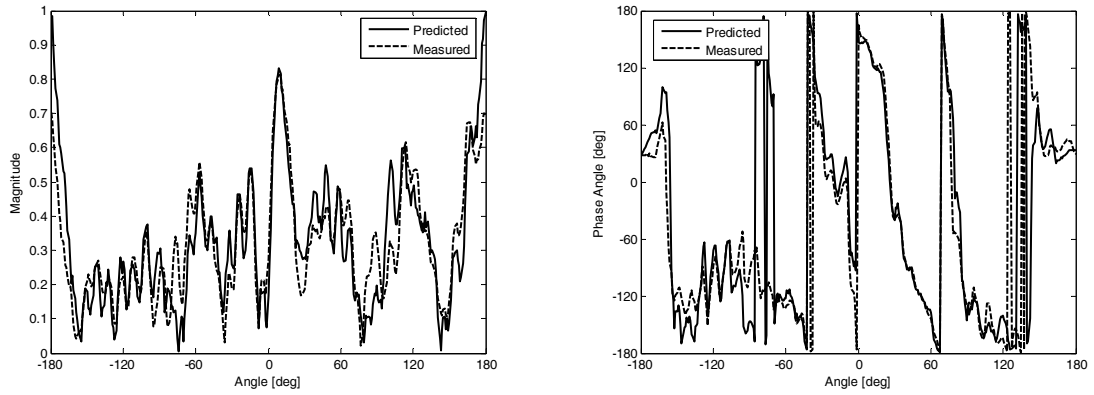

Figure 8: Predicted and measured pattern magnitude and phase when all elements in endfire mode

4.2 BPSK Example

The next example will illustrate BPSK communication. An angle was selected (-36° from broadside) where two sets of switch combinations produced two signals that were about the same magnitude and about 180° out of phase. The normalized complex constellation points are plotted in Figure 9, where they are normalized to the right point. If we let BBEE denote elements 1 and 2 in broadside mode and elements 3 and 4 in endfire mode, then the two modes that generated this BPSK constellation were EEEE and EEBE.

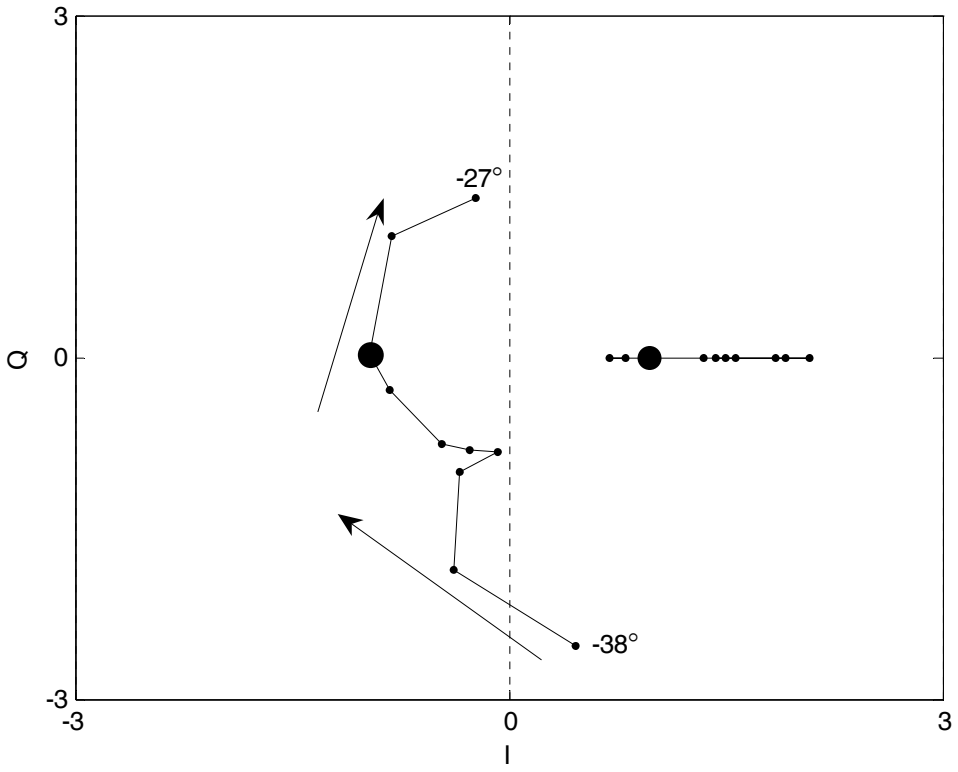

Figure 9: Calculated BPSK demonstration showing modulation beamwidth. Large circles are BPSK constellation points at -36° from broadside. Arrows go in increasing angle from -38° to -27° from broadside.

Another important illustration contained in this example is the concept of modulation beamwidth. Modulation beamwidth is defined as the range of angles through which a constellation can be demodulated without error by a receiver using a hard decision MMSE decoding scheme and no error-correction coding. For BPSK, this would mean deciding a symbol was a "1" when it is in the +I region in Figure 9 or a "0" when it falls in -I region. The path shown from -38° to -27° is what the constellation would look like to a receiver at each of those transmit angles. All points have amplitudes normalized to the same amount. At each angle, the constellation is rotated so one point falls on the positive x axis. Thus when toggling between these two modes of transmit, a receiver at

-27° would see two symbols with a phase difference of about 100°. It is then more difficult with the presence of noise and interference to demodulate the signal at -27° and beyond. The transmission has added security because it is spatially distorted toward directions not of interest. The modulation beamwidth is about 11°, which is the range of consecutive angles where the two BPSK points fall in opposite sides of the decision region. This is much smaller than the 54° first null beamwidth measured from this array when all elements are in broadside mode. Of course, a tradeoff is that gain is sacrificed to achieve security. Also, there may be other angles at which the modulation points are again in their correct sections for demodulation. These angles can be limited by using a higher order modulation scheme or by increasing the size of the array.

4.3 QPSK Example

The next example is a QPSK transmission at 34° from broadside. The four modes used to generate these signals were BEBE, BBEE, BEEE, and BBBE. All four had approximately the same signal amplitude and all shared a 90° phase difference in the patterns at the desired direction. The normalized constellation is shown in Figure 10.

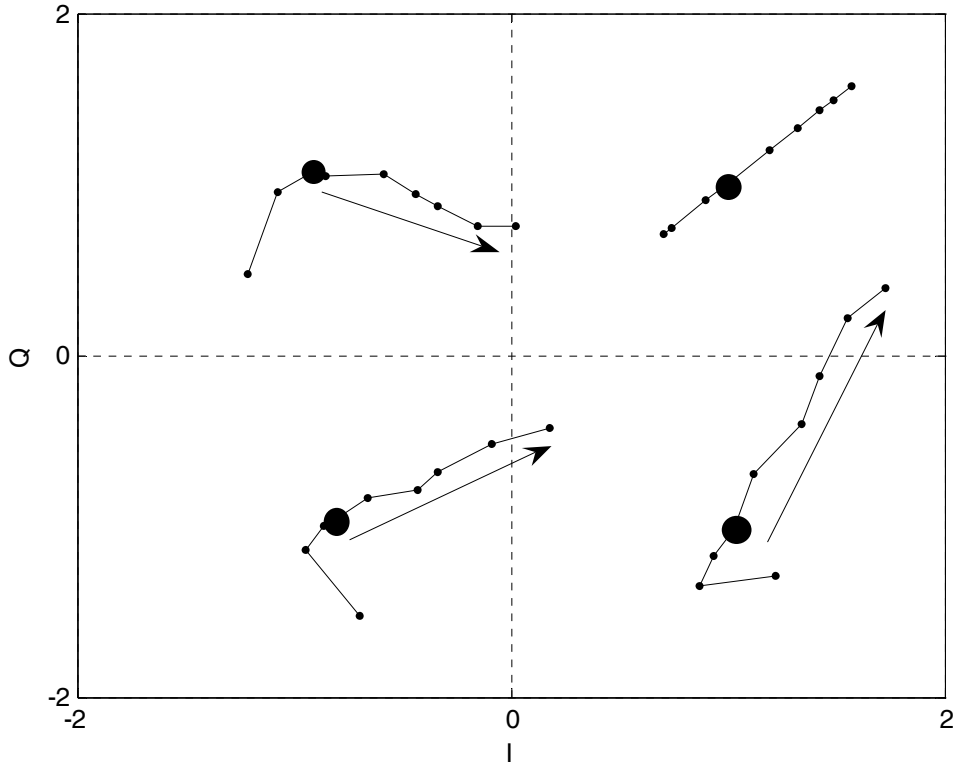

Figure 10: Calculated QPSK at +34° from broadside (large points). Arrows point in direction of increasing angle. Angles from 30° to 38° shown.

Once again, the progressive distortion of this constellation is shown by the lines and arrows for transmit angles moving off of the desired angle. There is a tradeoff between security and gain when using directional modulation. When using the antenna elements to create the modulation, power is wasted transmitting to other directions and the array gain will not be optimal. Figure 11 shows the radiation patterns for all four modes, and the transmit angle is delineated by an arrow. The electric field is anywhere from 6 to 12 dB less than the maximum pattern for the four modes, but without phase shifters this was the only means of obtaining the phase changes required for QPSK. Only limited beam steering can be accomplished by reconfigurable elements alone, and better performance can be achieved by either using more reconfigurable elements or phase shifters in the array. Of course, this reconfigurable array has limited beam steering (without phase shifters) when used in the conventional way as well.

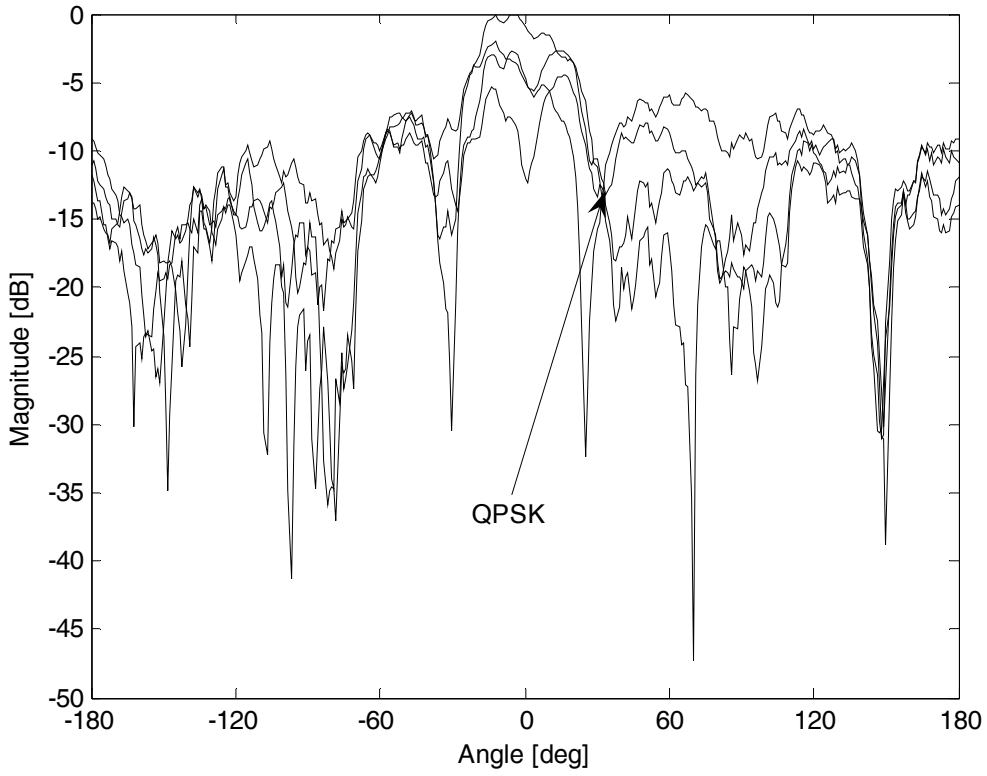

Figure 11: Measured radiation pattern magnitude at which QPSK is occurring relative to the mainlobes for all 4 QPSK points

Figure 12 shows the predicted improvement gained by using 1-bit phase shifters when transmitting QPSK at 34° from broadside. An optimization was carried out using a genetic algorithm that tested possible antenna modes and phase shifter combinations. Its

cost function had the goals of achieving a 90° phase differences between the four symbols in the transmit direction while maintaining uniform amplitude, maximizing the amplitude in the transmit direction, and minimizing the same phase differences transmitted in other directions. The third goal means that it is undesired to achieve a 180° difference between two of the symbols simply by toggling all phase shifters, because that will send the same phase difference out in all directions. The resulting best modes were found to be BBEB, BBEE, EEBB, and BBBB, with phases given in Table 1.

QPSK Point	Elt. 1 Phase	Elt. 2 Phase	Elt. 3 Phase	Elt. 4 Phase
45°	180°	0°	0°	0°
135°	0°	0°	180°	180°
225°	0°	180°	180°	0°
315°	180°	180°	0°	180°

Table 1: Respective phase shifts for each of the 4 QPSK symbols

The constellation in Figure 12 exhibits good amplitude and phase agreement for QPSK. The signal magnitude relative to other directions is still not at a peak but is no longer -12 dB down like in Figure 11. The signal power in the transmit direction increased approximately 3 dB by use of 1-bit phase shifters. Clearly, when an array has more ways to reconfigure, it can more easily achieve desired modulations while maximizing amplitude.

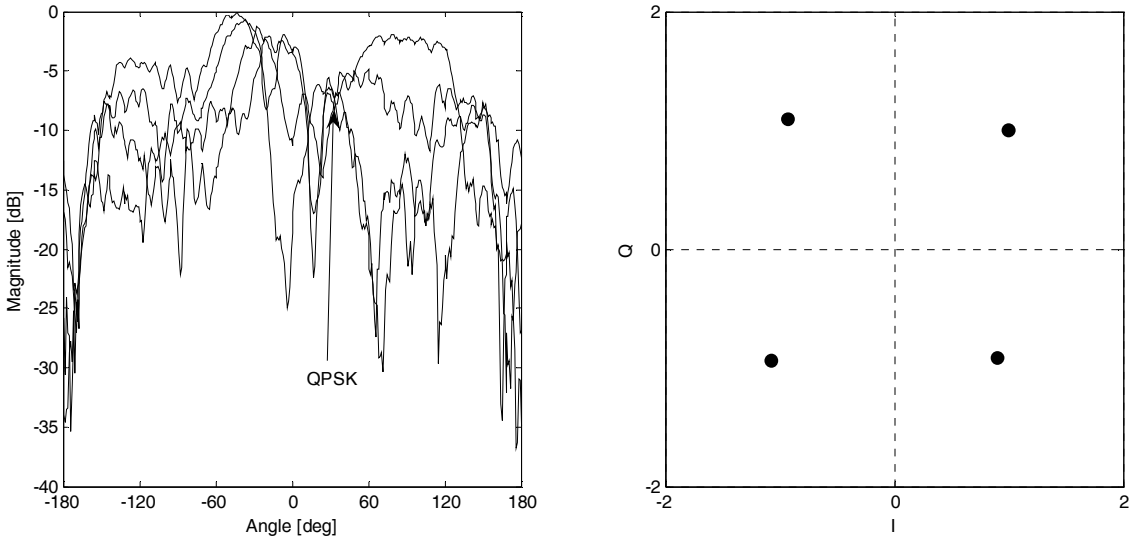

Figure 12: Calculated patterns of array using 1 bit phase shifters transmitting QPSK at 34° (left) and constellation diagram at transmit angle (right)

4.4 QAM Example

The final example shows a pseudo-QAM constellation with both calculated and measured points. It is "pseudo-QAM" because it does not exactly conform to any specific QAM constellation but serves to show that even with only 16 possible modes, a good diversity of phases and amplitudes can be achieved in some directions. It also serves to show how the measured constellation points compare with the predicted points. Besides taking full patterns for BBBB and EEEE modes, patterns were also measured for BEBE and BEEB modes shown in Figures 13 and 14. Even when intermixing the elements in broadside and endfire configurations, the radiations patterns of these modes were accurately predicted by the superposition of broadside and endfire active element patterns. Thus, the mutual coupling effects of the neighboring elements were approximately the same whether those neighboring elements were in broadside or endfire mode.

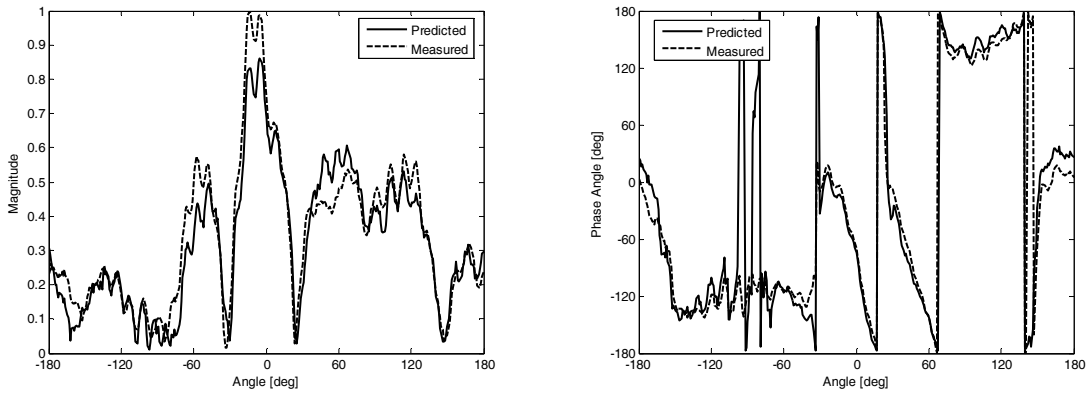

Figure 13: Predicted and measured patterns for BEBE mode

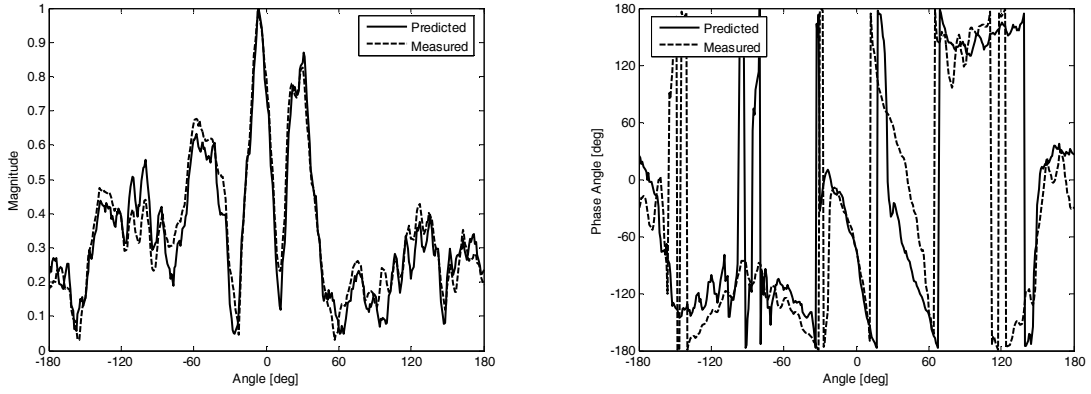

Figure 14: Predicted and measured values for BEEB mode

Figure 15 shows all 16 combinations at +27° from broadside. The constellation is normalized so one of the sixteen modes falls at the coordinate (I,Q)=(1,1). The four crosses show the measured results at +27° from the four measured modes. The

amplitudes and phases of these calculated points agree well with their measured counterparts. Even with an array only capable of 16 modes, the signals are spread out in amplitude and phase showing how higher order PSK and QAM modulations are possible even with simple arrays. Additional elements or phase shifters provide more freedom to adjust individual constellation points to achieve higher order modulations.

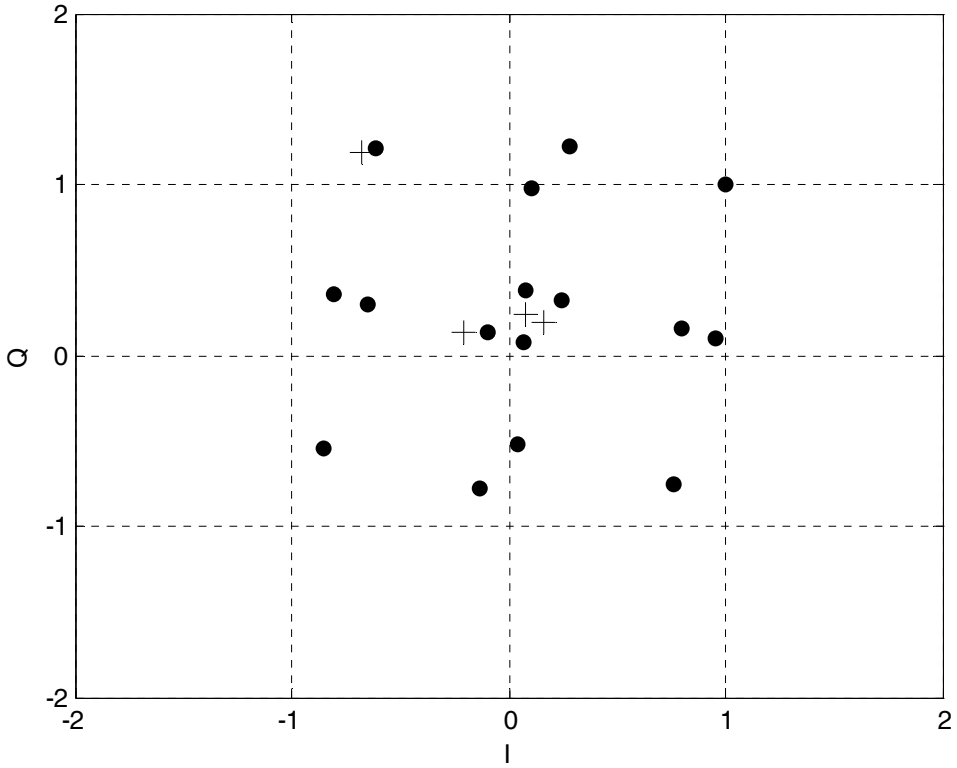

Figure 15: "QAM" constellation at +27° from broadside. All 16 calculated switch combinations shown (dots) and 4 measured (crosses)

5. Conclusion

Directional modulation with a reconfigurable array of driven elements has been demonstrated. It was shown that using solely element patterns, constellation diagrams could be accurately predicted without measuring each combination or using an electromagnetic solver. Instead of having to measure all possible switch combinations, only each element need be measured in both of its modes. This takes the problem complexity from exponential to linear. Also, the security of this technique was demonstrated by showing how the constellations become distorted away from the intended angle of transmission. By increasing the number of elements or the degrees of freedom in changing their patterns, more difficult tasks such as independent communications in multiple directions can be achieved.

6. References

[1] W. H. Kummer, A. Villeneuve, T. Fong, and F. Terrio , "Ultra-low sidelobes from time-modulated arrays," *IEEE Trans. Antennas Propag.*, vol. 11, pp. 633–639, 1963.

[2] B. L. Lewis and J. B. Evans, "A new technique for reducing radar response to signals entering antenna sidelobes," *IEEE Trans. Antennas Propag.*, vol. 31, pp. 993–996, 1983.

[3] S. Yang, Y. B. Gan, P. K. Tan, "Linear antenna arrays with bidirectional phase center motion," *IEEE Trans. Antennas Propag.*, vol. 53, pp. 1829–1835, May 2005.

[4] E. Baghdady, "Directional signal modulation by means of switched spaced antennas," *IEEE Trans. Communications*, vol. 38, pp. 399–403, Apr. 1990.

[5] C. M. Elam and D. A. Leavy. Secure communication using array transmitter. U.S. Patent 6,275,679, Aug. 14, 2001.

[6] A. Babakhani, D. B. Rutledge, and A. Hajimiri, "A near-field modulation technique using antenna reflector switching," *IEEE International Solid State Circuits Conference*, pp. 188–189, 605, Feb. 2008.

[7] C.A. Balanis, *Antenna Theory: Analysis and Design*, 3rd ed., Hoboken, NJ: John Wiley & Sons, 2005, ch.6.

[8] G.H. Huff and J.T. Bernhard, "Integration of packaged RF MEMS switches with radiation pattern reconfigurable square spiral microstrip antennas", *IEEE Trans. Antennas and Propag.*, vol 54., Feb. 2006, pp. 464-469.

[9] K. Hietpas, "Beam steering in phased arrays using a pattern-reconfigurable antenna," M.S. Thesis, University of Illinois at Urbana-Champaign, Urbana, IL, 2004.